



TECHNOLOGY DEVELOPMENT FOR EXOPLANET MISSIONS

*Technology Milestone White Paper
Colloid Thruster Life Testing and Modeling*

*Colleen Marrese-Reading (JPL, Caltech), P.I.
Steven Arestie (JPL, Caltech), Nathaniel Demmons (Busek Co.),
Manuel Gamero-Castaño (University of California, Irvine)*

June 10, 2024

*National Aeronautics and Space Administration
Jet Propulsion Laboratory
California Institute of Technology
Pasadena, California
©2024 copyright. All rights reserved*



Approvals:

Released by

Colleen Marrese-Reading
Principal Investigator

Date

Approved by

Brendan Crill
ExEP Deputy Program Chief Technologist

Date

Nick Siegler
ExEP Program Chief Technologist

Date

Lucas Paganini
ExEP Program Executive, NASA-HQ

Date

Table of Contents

1	Objective	4
2	Introduction/Background	4
	2.1 Colloid Micronewton Thruster (CMT)	5
	2.2 CMT Performance	6
	2.3 CMT Beam Model	7
	2.4 CMT Life Model.....	8
3	Milestone Definition	11
4	Experiment Description	12
	4.1 Single Emitter Assembly Electrode Wear Rates	13
	4.2 Beam Measurements.....	14
	4.3 Thruster Electrode Wear Rate Measurement and Lifetime Estimate	15
5	Data Measurement & Analysis.....	16
	5.1 Single Emitter Assembly Electrode Wear Rates	16
	5.2 Beam Measurements.....	17
	5.3 Thruster Electrode Wear Rate Measurement and Lifetime Estimate	17
	5.4 Lifetime Model Validation.....	18
	5.5 CMT Design Validation	18
6	Success Criteria.....	19
7	Certification.....	20
	7.1 Milestone Certification Data Package.....	20
8	Schedule.....	20
9	Acknowledgements	21
10	References.....	21

TDEM Milestone White Paper

Colloid Thruster Life Testing and Modeling

1 Objective

The objective of this task is to demonstrate that the Colloid Micronewton Thruster (CMT) has a > 7.5 year lifetime capability with 95% statistical confidence for TRL 5 qualification by long duration testing and analysis with a validated lifetime model.

2 Introduction/Background

The National Academy of Sciences' 2021 Decadal Survey Report recommends that an IR/Visible/UV (IROUV) Great Observatory capable of imaging exoplanets should be NASA's highest priority for the next decade or more [1], and life testing colloid microthrusters was one of 8 areas that required significant attention. To image exoplanets, observatory and contrast stability is a key requirement and has been identified as a Tier 1 priority in the Exoplanet Exploration Program (ExEP) Technology Gap List [ExEP Technology Gap List]. It states that contrast and observatory stability can be addressed with ultra-stable structures and disturbance isolation and reduction using flight-proven colloid thrusters [2]. The colloid thruster high precision thrust and thrust vector stability enabled the extraordinary performance of the ST7-Disturbance Reduction System (DRS) to control the ESA/NASA LISA Pathfinder (LPF) spacecraft to nanometer position stability [3]. The HabEx study report provides the required instrument contrast for the coronagraph of 10^{-10} to observe exo-Earths, which demands line-of-sight pointing stability ≤ 2 mas RMS per axis [4]. HabEx baselined the colloid microthrusters, to achieve telescope stability because, "without reaction wheels, HabEx's self-induced jitter is essentially nonexistent." An independent study by the NASA Engineering and Safety Center, "Application of Micro-Thruster Technology for Space Observatory Pointing Stability," has shown that colloid thrusters on segmented and monolithic mirror telescopes achieved 10x better pointing stability performance than Hubble Space Telescope, which is required for imaging exoplanets, while reaction wheels alone cannot [5]. A study using thrusters-only ACS with colloid electro-spray microthrusters on a 6 Meter Space telescope showed that the 2 mas 1-sigma pointing stability requirement can be readily achieved and could be feasible for missions like the Habitable Worlds Observatory (HWO) [6].

HWO will operate for ≥ 4 years and will require continuous colloid thruster operation for days to weeks at a time during exoplanet imaging observations, requiring an accumulated lifetime of at least 35,040 hours for the nominal mission with enough propellant for more than a decade. A 9 emitter, 5-30 μN Colloid Micronewton Thruster (CMT), that was developed by the company Busek, has been demonstrated in ground testing for 3,458 hours [7] and in the ST7-DRS payload on the LPF Mission for >2,400 hours [3,8]. Physics-based models of failure modes and lifetime predictions, developed recently under the NASA LISA Study Office (NLSO), show that the much longer mission lifetime needs can be met for the Busek CMT design that was recently improved, from the ST7 CMT, for longer lifetime [9]. With the CMT performance already proven in flight, demonstrating lifetime capability, of this recently improved design, is the key remaining technology development challenge, and the objective of this task.

This Colloid Thruster Life Testing and Modeling Task was funded by the Strategic Astrophysics Program, to perform a long-duration Colloid Micronewton Thruster (CMT) test at Busek to validate the thruster design and lifetime model, using the demonstration model (DM) thruster and feed system hardware developed under the NLSO. The thruster design has recently been improved for longer lifetime

NASA science missions. The thruster design and lifetime model are highly scalable for any number of emitters to meet any mission thrust and lifetime requirements, and this scalability and thruster wear rate predictability will be verified in this task with testing and model validation at both the single electro spray emitter and 9 emitter electro spray thruster head configurations. By the end of this task, a thruster lifetime model will have been experimentally validated with a long duration test for a 9-emitter thruster, and with the single emitter tests, it will have been validated to be scalable to any number of emitters in a thruster head. The lifetime model can then be used to both design a thruster for the required lifetime for a specific mission profile and predict the lifetime of a specific thruster design. A long duration thruster test in this task for 4000-8000 hours with acceptable and predictable performance and wear rates should be sufficient to qualify the technology to a TRL 5 with the environmental tests already conducted. Alternatively, a project could support the continuation of the long duration test with model and model scalability validation to follow the completion of it.

2.1 Colloid Micronewton Thruster (CMT)

The Busek Colloid Micronewton Thruster (CMT) is a highly scalable micronewton electro spray thruster capable of precision thrust with low thrust noise [10]. An illustration of the electro spray process and elements are shown in Fig. 1. The propellant is the ionic liquid EMI-Im (1-ethyl-3-methylimidazolium bis(trifluoromethylsulfonyl)imide) [11]. The CMT was successfully flight qualified and demonstrated on ST7 with this propellant. The liquid propellant is pressure-fed through the capillary emitter and electro sprayed into charged droplets and ions by setting a voltage difference between the emitter and an extractor electrode, that is typically 1600 V. The charged particles are accelerated towards and through a concentric aperture in the extractor by the electric field. They are further accelerated and focused by the accelerator electrode, also with an orifice that is concentric with the emitter and biased to -1 kV to prevent electron back-streaming to the emitter. The emitter is biased to 2 - 8 kV. The high voltage between the emitter and the accelerator results in beam focusing that increases with voltage between them. The thrust level is scalable with number of emitters in the thruster head. A cut-away model of the CMT it is shown in Fig. 2. The breadboard thruster design, shown in Fig. 3, was built and demonstrated by Busek Co., Inc. with NSLO funds.

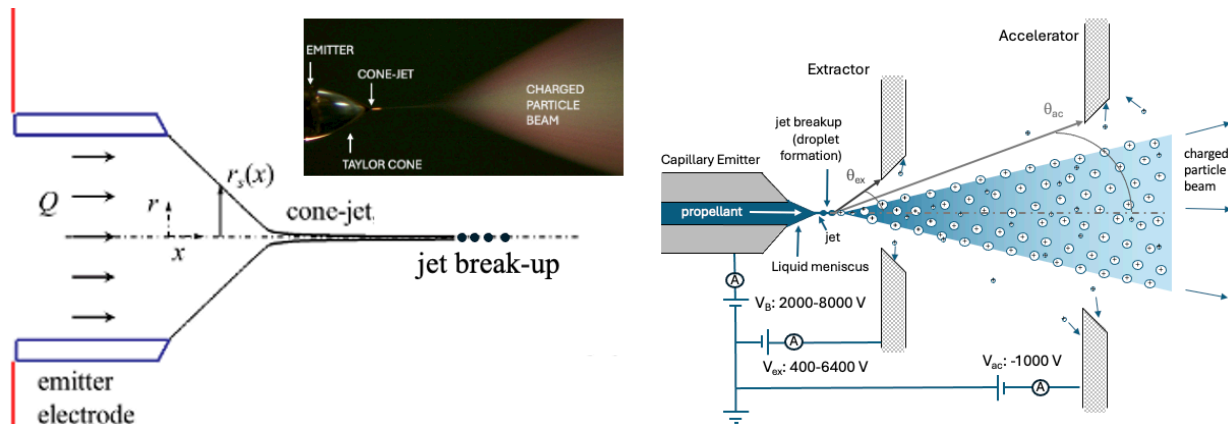


Fig. 1. Electro spray image [12] and illustrations of the electro spray cone-jet and the CMT electrode configuration and operating voltages.

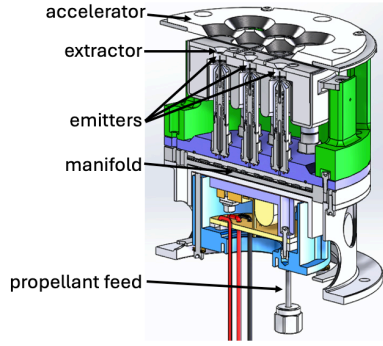


Fig. 2. CMT cut-away CAD model.



Fig. 3. Breadboard CMNT hardware.

2.2 CMT Performance

The thruster performance is highly predictable with verified performance on the ground and in flight. The functional form of the colloid thruster thrust model is given in Eqn. 1 [13]. It provides the relationship between thrust level, T (microNewtons), the beam current, I_B (microAmperes), applied beam voltage, V_B (Volts), and thrust coefficient, C_1 , as defined in Eqn. 2. V_{tc} is a voltage drop across the Taylor cone jet between the emitter electrode at the beam voltage and the charged particle emission site. C_1 depends on the properties of the propellant in the α term, given in Eqn. 3, and multiple efficiency factors of the thruster (i.e. propellant utilization, grid impingement, beam spreading, and non-uniform charge-to-mass ratio distribution), where m/q is the charged particle mass-to-charge ratio and I_n is a single emitter current. The critical properties of the propellant depend on temperature and water content. They include propellant density, ρ , dielectric constant, κ , conductivity, σ , surface tension, γ , and a function, $f(k)$ that depends on the dielectric constant and the number of emitters, N . The current supply efficiency, η_{curr} , is the ratio of the current of charged particles in the beam to the current measured to the emitters. The grid current interception efficiency, η_{grid} , takes into account the beam current that is intercepted by the extraction and acceleration electrodes and does not produce thrust. The beam spread efficiency, η_{spread} , is the ratio of the actual thrust produced by the beam to the ideal thrust from that beam without any beam divergence. The charge-to-mass-ratio efficiency, $\eta_{q/m}$, is related to the emitters producing charged particles with a distribution of charge-to-mass ratios that are accelerated to different velocities.

$$T = C_1 I_B^{\frac{3}{2}} (V_B - V_{tc})^{\frac{1}{2}} \quad (1)$$

$$C_1 = \frac{\alpha}{\sqrt{N}} \eta_{curr} \sqrt{\eta_{grid} \eta_{spread} \eta_{q/m}} \quad (2)$$

$$\alpha \equiv \sqrt{\frac{2}{I_n} \left\langle \frac{m}{q} \right\rangle} = \sqrt{\frac{\rho \kappa}{(f(\kappa))^2 \sigma \gamma}} \approx f(temp) \quad (3)$$

ST7-DRS used a simplified version of the performance model with V_{tc} set to 0 V for thruster control that was validated on a thrust stand [14]. Thrust was measured in the 5-30 μN range to estimate the thrust coefficient, C_1 . With this simplified version of the performance model, the delivered thrust was achieved within 2% of the commanded thrust at nominal voltages, currents and temperature and with a C_1 of 0.0319. The values of C_1 at different temperatures have been predicted using models including the physical properties of the propellant and verified by measurement [10,15]. The C_1 values estimated from ground measurements are 0.0372 at 15°C, 0.0343 at 20°C, 0.0298 at 30°C. They were used in the thruster control algorithm for the flight experiments at these temperatures and validated in flight [2,16]. The thruster temperature on ST7 was controlled to 25°C. Because the propellant is hygroscopic, it must be dried to achieve the required water content at ≤ 150 ppm for this performance model.

2.3 CMT Beam Model

The CMT beam model is a steady and axisymmetric electro-spray beam model that propagates the charged particles electro-sprayed from a single emitter to and through the electrodes and downstream of them determining the expansion of the charged particle mass and current profile throughout the plume [17]. The beam model includes both charged droplets and molecular ions. Inputs to the beam model include the experimentally measured distribution of diameters and charge-to-mass ratios of the droplets and their initial position, velocity and potential. The beam expansion model computes the trajectories of charged droplets forced by the electric field resulting from the combination of both the potentials applied on electrodes and the distribution of charges within the beam [12]. The electric field acting on the charged droplets is the solution of the Poisson equation. Unlike previous calculations in which the electric field is approximated as the sum of the field generated by the electrodes in the absence of space charge, and the field of the space charge in the absence of electrodes [18] this model solves the Poisson equation without this decoupling approximation. Any arbitrary electrode geometry can be resolved, including the triode (emitter, extractor and accelerator) configuration. The expansion of electro-spray beams is dominated by Coulombic repulsion of the droplets in an initial region following the emission point. This initial region is small compared to the characteristic lengths of the electrodes such as the gaps between the emitter, extractor and accelerator electrodes, and the diameters of the emitter and the orifices of the extractor and accelerator. The model takes advantage of this feature by dividing the beam into two successive regions where the trajectories are solved in different ways: an inner region near the jet breakup where the trajectories of individual charged droplets are integrated simultaneously, and where Coulomb repulsion between droplets is fully calculated while integrating the equations of motion; and an outer region where the structure of the beam is obtained by first dividing the distribution of droplets into a finite number of subfamilies of equal charge-to-mass ratio, further dividing the total current of each subfamily into fractions, and computing the envelopes enclosing each current fraction [18]. The solution of the inner region is used to compute the initial conditions (initial position and initial angle of the envelopes) for the outer region problem. Additional coupling between the two regions is provided by the combined space charge, and its effect on the electric field. The inner region solves Newton's equation of motion for individual charged droplets, where the electric field is obtained from the solution of Poisson's equation. Note that the initial position and velocities of the droplets are taken to be the average position at which the jet breaks up. The velocity and potential of the jet at the breakup are key inputs in the model, and can be measured with an experimental technique based on the characterization of both the retarding potential and the charge-to-mass ratio of individual droplets (or families of droplets) [19]. They will be measured in this task. They have been estimated for the current version of the model. The charged droplets are sequentially introduced in the computational domain, simulating the jet breakup. The diameter and charges of the droplets in this sequence are obtained from existing charge to mass ratio distributions measured with the time-of-flight technique, combined with the assumption of a Gaussian diameter distribution and a charge level of 68% of the Rayleigh stability limit [20]. When creating this sequence of droplets, the condition is enforced that the current associated with a small sequence of droplets equals the current of the electro-spray beam. The space charge is the main driving force for the initial expansion of the beam.

The model output includes the ion and charged droplet current and mass distribution in the plume with polar angle. The model has been validated against experimental data from UCI. Beam propagation simulations have been conducted for many beam current and voltage cases to create a surrogate model of the data that has been used by the thruster life model. The beam model is in the process of being integrated into the life model to run together in the simulations. The beam model results have been compared to experimental results at JPL. The beam model is predicting no current or much lower currents to the extractor and accelerator electrodes than have been measured at JPL through the nominal current and voltage range. It is understood that ions can evaporate off of the droplets and charged particles can

undergo coulombic explosions in flight that will result in broadening of the beam and higher charged particle currents to the electrodes [21]. The significance of these physical processes and their impact on thruster lifetime will be investigated in this task and added to the beam model if necessary. Also, the model will be improved with measurements of the velocity and potential of the jet at the breakup with single emitter assembly with the CMT electrode geometry and nominal current and voltages.

2.4 CMT Life Model

The thruster lifetime model developed by JPL, Busek, University of California, Irvine (UCI) and University of California, Los Angeles (UCLA) [22, 23] includes several sub-models and a surrogate model of physical phenomena that impact thruster lifetime including the beam and thruster performance model discussed in the previous sections. The model is based on the dominant lifetime limiting mechanism, which is propellant deposition into the porous extractor and accelerator electrodes (termed “overspray”), as shown in Fig. 4. It illustrates the electrode and beam configuration and the overspray and back-spray processes. Fig. 5 shows the porous stainless steel extractor and accelerator material structure for absorbing propellant sprayed at it. The extractor accumulates propellant at a faster rate than the accelerator; therefore, it has been designed with a larger capacity to absorb propellant. The lifetime model elements and framework are illustrated in Fig. 6. The lifetime model simulation uses the Sandia Dakota software to translate model parameter uncertainties into electrode wear rate/lifetime confidence intervals. [24] The model validation elements and model flow with Dakota are illustrated in Fig. 7. The **performance model** calculates current and voltage from a thrust level input using Eqns. 1-3 and other conditions that determine and limit V_b , depending on the feed system response time and mission requirements [16]. The **backspray model** is simply represented by the condition that backspray begins when the electrodes are 95% full, defining the lifetime at 95% full electrodes. Experiments have revealed that when the electrodes have been filled to >95% capacity, back-spray begins between them because the propellant can electro-spray in positive and negative charged particle emission modes. When significant backspray ensues, controllable lifetime of the thruster has been exceeded as thrust noise increases and current and thrust control is compromised [9,25]. The single emitter test at the End-of-Life (EOL) condition in this task will reveal whether this process requires a higher fidelity model and whether it significantly affects the electrode propellant loading rates and, therefore, thruster lifetime. The **porous grid** model includes the condition that if propellant is intercepted by the extractor or accelerator, it is absorbed by it, because experiments revealed that the electrodes can absorb propellant at rates that exceed the expected rates. The **flow system model** is still under development to determine how or whether the feed system performance will impact lifetime. Testing of the existing flow system will be conducted in the beginning of the task at Busek to characterize the performance of it with a thruster head and then develop a model of it before the Thruster String Assembly (TSA) cleaning and assembly for the long duration test. The flow system model will include the expected flow rate response to the commanded thrust level, beam voltage and corresponding current and propellant flow rate, based on experimental results. Only Busek has a feed system that is relevant for the flow model development. It is not necessary for the experiments at JPL and UCI. The **facility effects model** is under development at JPL. It will be available for integration into the lifetime model before the Lifetime Model Review and Test Readiness Review in 2024. It will include 1) the mass flux back to the electro-spray source/thruster from the facility beam target as a function of beam current and voltage and 2) the impact of facility pressure on beam divergence.

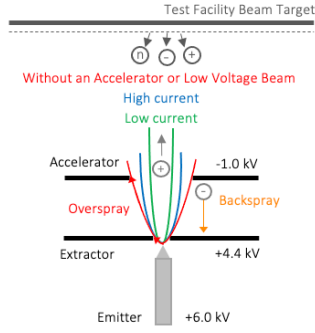


Figure 4. Single emitter electro spray beam, electrode and beam target configuration.

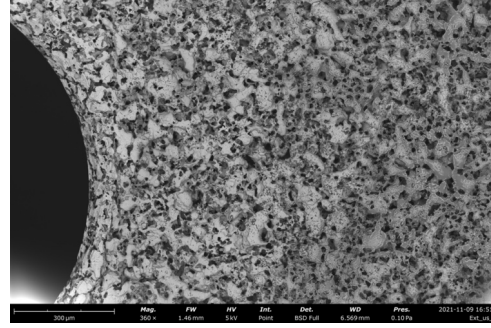


Figure 5. A scanning electron micrograph of the porous electrode material to absorb the propellant overspray to the electrodes.

Estimating the mass flow rate of propellant to the extractor and accelerator electrodes at any thrust level, temperature, electrode geometry and with any number of emitters then includes calculating the 1) thruster beam current, I_b , and voltage, V_b with the performance model, 2) the current per emitter, I_b from the beam current, I_b , and number of emitters, $N_{emitters}$, 3) the mass distribution in the plume at the extractor and accelerator with the beam model, $\Phi_{mac}(\theta)$ and $\Phi_{mex}(\theta)$, and then 4) the propellant mass flow rate into the extractor and accelerator. The extractor and accelerator electrode beam interception angles depend on the propellant cone meniscus height above the emitter needle, h_m , which varies with emitter beamlet current, I_b , as modeled by Eqn. 4. UCLA developed this model from meniscus imaging and height measurements in the current range of 310-710 nA [26],

$$h_m = mI_b + c, m = (0.043 \pm 0.005)\mu m nA^{-1}, c = (42.95 \pm 2.8)\mu m. \quad (4)$$

The propellant mass flow rate to the accelerator electrode is calculated by integrating the mass flux data between the accelerator and extractor interception angles and to the extractor by integrating the mass flux data between the extractor interception angle and 60° . The accelerator interception angle, θ_{ac} , the extractor interception angle, θ_{ex} , the mass flow rate to the accelerator, \dot{m}_{ac} , the mass flow rate to the extractor, \dot{m}_{ex} , are estimated as follows, with the diameter of the extractor and accelerator aperture, $dapAc$ and $dapEx$, the concentricity of the accelerator and extractor, $cncAc$ and $cncEx$, the distance to accelerator and extractor, zAc and zEx , the thickness of the aperture in the accelerator and extractor, $tapAc$ and $tapEx$:

$$\theta_{ac,ex} = \text{atan} \left(\frac{\left(\frac{dapAc,Ex}{2} \right) - cncAc,Ex}{zAc,Ex - h_m + tapAc,Ex} \right) \quad (5)$$

$$\dot{m}_{ac} = \int_0^{2\pi} \int_{\theta_{ac}}^{\theta_{ex}} \Phi_{mac}(\theta) r^2 \sin \theta d\theta d\phi \quad (6)$$

$$\dot{m}_{ex} = \int_0^{2\pi} \int_{\theta_{ex}}^{60} \Phi_{mex}(\theta) r^2 \sin \theta d\theta d\phi \quad (7)$$

The total propellant flow rate to the accelerator and extractor, \dot{m}_{actot} and \dot{m}_{extot} , can be summed for any number of emitters, $N_{emitters}$, in the thruster head and then the lifetime can also be determined at that thrust level with the mass capacity of the accelerator and extractor, m_{accap} and m_{excap} as follows:

$$\dot{m}_{ac,extot} = \sum_{N=1}^{N=N_{emitters}} \dot{m}_{ac,exN} \quad (8)$$

$$t_{ac,exlife} = \frac{m_{ac,excap}}{\dot{m}_{ac,extot}} \quad (9)$$

However, a mission will include many thrust levels during science mode operations or continuously changing thrust levels so that the total mass deposited into the electrodes, $\Delta m_{ac-scimode}$ and $\Delta m_{ex-scimode}$ can be summed up over all thrust levels and the time at each thrust level for any specific mission thrust profile,

$$\Delta m_{ac,ex-scimode} = \sum_0^{N=N_{thrustlevels}} \dot{m}_{ac,ex}(T_N) \Delta t_N. \quad (10)$$

Transient operating modes during first start-ups during commissioning and every subsequent start-up and shutdown are not yet captured in the lifetime model. They will also contribute to propellant mass deposition in the electrodes. While they will consume very little of the mission timeline, they could contribute significantly to the electrode wear rates. They will be characterized and modeled in this task with single emitter testing and included in the thruster long duration test.

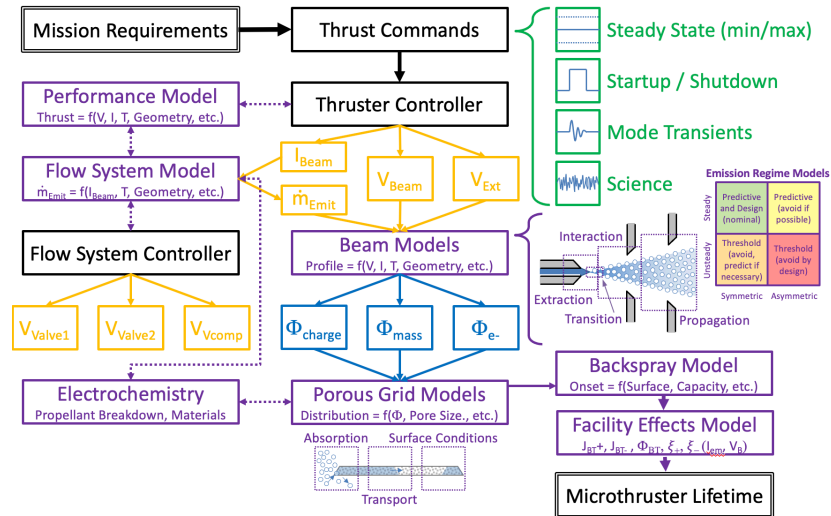


Figure 6. Life model elements and framework.

The life model parameter uncertainty inventory used by Dakota includes all of the parameters used in the model with their known or estimated distributions, uncertainties or discrete values. They include extractor and accelerator electrode fabrication and assembly alignment tolerances, experimental measurement errors and could include a thrust level distribution for a simulation. The fabrication and alignment tolerance requirements were developed to minimize the beam current intercepted by the electrodes. [25]

Preliminary lifetime modeling results in steady operating modes suggest a thruster lifetime greater than 10 years at 5-30 μN with 9 emitters [9]. Long duration single emitter test results suggest a thruster lifetime greater than 7.5 years at 5-30 μN with 9 emitters, although they demonstrated a much higher wear rate than the models are predicting. Current lifetime estimates from experimental and modeling results in steady operation at a constant thrust level are in Fig. 8. The discrepancies are expected to be due to transient phenomena and/or droplet breakup, field emission of ions off of droplets and charged particle interactions downstream of the emission site. Model improvements and experiments will address the differences between the modeling and experimental results to improve agreement. Because emitters do not influence each other, the thruster lifetime depends on the maximum required thrust and current per emitter, with number of emitters and porous electrode capacity expected to be scalable to meet any thrust and lifetime requirement. This technology scalability will be demonstrated with the single emitter electro spray and 9 emitter electro spray thruster test.

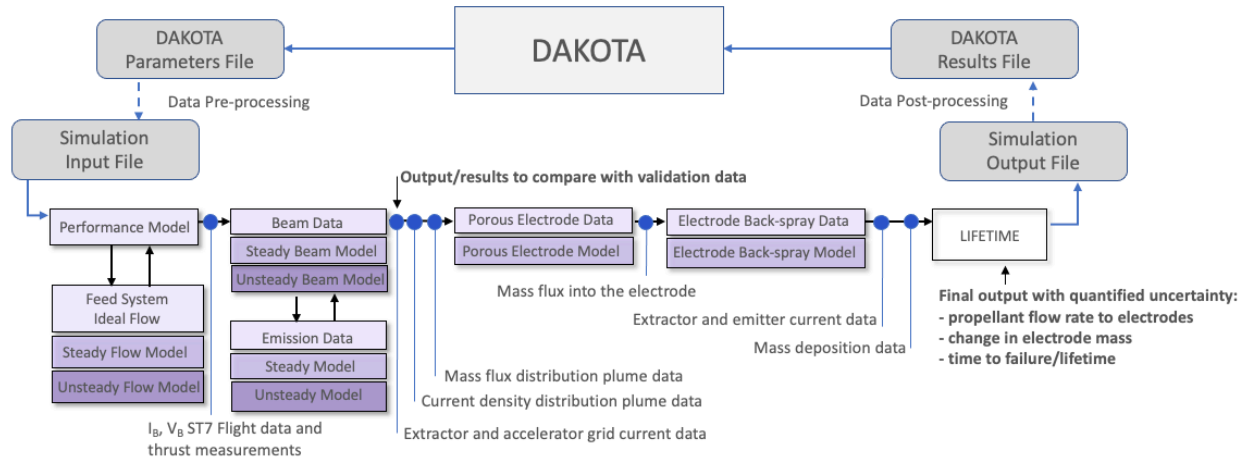


Figure 7. Microthruster life model simulation flow with Dakota for uncertainty quantification, showing where test data provides model element validation.

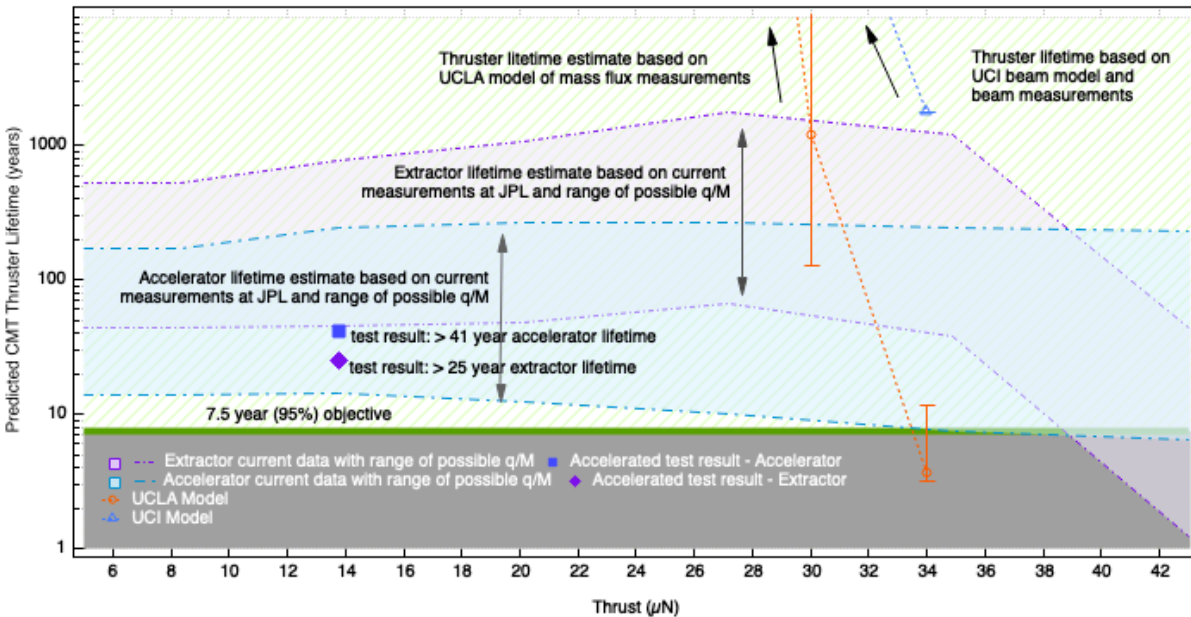


Figure 8. JPL integrated UCI modeling results and UCLA measurement results into the steady thruster lifetime mode, with uncertainty quantification, to provide a prediction of thruster lifetime. The thruster lifetime predicted with the UCLA model of measurements and UCI beam model that includes measured parameters, including uncertainty, suggest >7.5 years at $\leq 30 \mu\text{N}$, as shown on the graph, for a 9-emitter thruster. Maximum thrust scales linearly with number of emitters. Lifetime decreases significantly at higher thrust levels for this 9-emitter thruster above $30 \mu\text{N}$. Longer lifetime at higher thrust levels requires more emitters to decrease the current per emitter.

3 Milestone Definition

Validate the Colloid Micronewton Thruster (CMT) technology lifetime capability of 7.5 years with a 95% confidence interval by analysis and test with a long duration life test to achieve a critical TRL 5 success criterion.

This milestone will be achieved by the following sequence of demonstrations that include experiments and modeling:

1. Single emitter assembly tests revealing wear rates less than 6.4 $\mu\text{g}/\text{h}$ to the extractor and $< 2 \mu\text{g}/\text{h}$ to the accelerator electrode to be commensurate with >7.5 year lifetime through nominal thruster current and voltage ranges, at multiple conditions.
2. Single emitter assembly tests revealing wear rates commensurate with >7.5 year lifetime in unsteady transient operating modes for relevant mission durations. It includes $<5 \mu\text{g}/\text{on-off cycle}$ to the accelerator and extractor. It includes $<3.8 \text{ mg}/\text{h}$ to the extractor and $< 1.2 \text{ mg}/\text{h}$ to the accelerator in bubble shedding mode on first start-up.
3. A long duration thruster test with a goal of 4000-8000 hours demonstrating stable performance and a wear rate commensurate with >7.5 year lifetime. It requires that the remaining capacity of the extractor exceeds an estimated 55% (after 4000 hours) or 52% (after 8000 hours) and the accelerator exceeds an estimated 49% (after 4000 hours) or 46% (after 8000 hours) at the end of the test.
4. Thruster lifetime model validation with single electrospray emitter assembly and thruster test result agreement within $1-\sigma$ confidence interval.
5. Thruster design lifetime validation for >7.5 years mission by analysis.

A comprehensive testing and modeling program is required to demonstrate the thruster technology at TRL 5 and lifetime capability for observatory missions for > 4 years through all operating thruster modes and the scalability of it. Technology validation for 4+ year missions at TRL 5 requires a lifetime model with uncertainty quantification that has been validated experimentally at beginning and end of life conditions. It also requires understanding the impact of operating in steady and transient modes on thruster lifetime. The thruster test will be conducted through steady and transient modes, with an electrode mass change measurement after the long duration test. It may not be possible to deconvolve the contributions of each operating mode on the electrode mass deposition in the thruster electrodes. Therefore, separate steady and transient mode tests will be done with single emitter electrospray assemblies to measure mass loading rates in steady and unsteady transient modes. The wear rate of the electrodes in the single emitter assembly and in the thruster is the rate at which the porous electrode open volume becomes filled with propellant overspray from the beam. It will be measured in single emitter tests with the same electrode geometry as the thruster that has 9 emitters for life model validation. It will be measured at multiple current levels and in steady and transient modes in several separate tests. The thruster test duration goal is to be conducted for a duration that significantly exceeds the previous CMT life test and for wear rate measurement uncertainty of 0.1 mg to be less than 1% of the minimum electrode mass change measurement of 10 mg. This test duration goal could be as long as 8000 hours, based on estimated electrode wear rates. The single emitter tests will be conducted for hundreds of hours to achieve electrode mass change measurements that significantly exceed the 10 microgram measurement resolution capability. The single emitter and thruster test results will be compared to demonstrate scalability of the design and then they will be compared to the modeling results for model validation. Successful model validation requires that the modeling results agree with the experimental results within a $1-\sigma$ confidence interval. The thruster design will be validated for mission applications by the modeling results suggesting a 7.5+ year lifetime with a 95% confidence interval for a mission thrust profile and the experimental results suggesting a 7.5+ year lifetime for the conditions tested with both the single emitter and thruster assemblies.

4 Experiment Description

Three different experimental campaigns will be conducted in this task to validate the thruster technology and design for a lifetime that is several years beyond the long duration thruster test length. Single emitter assembly long duration experiments will be done at JPL to measure electrode propellant

mass loading rates, where similar tests have been conducted previously, to support the thruster life model validation. Electro spray beam measurements will be conducted at UCI to support the beam model development for the thruster life model. The long duration thruster test will be conducted at Busek, where thruster testing has been on-going during the development, and where a 3,458 hour CMT test was conducted previously for the LISA Pathfinder/ST7 mission.

4.1 Single Emitter Assembly Electrode Wear Rates

A temperature controlled single emitter electro spray with the CMT electrode geometry for the emitter, extractor and accelerator will be used to measure electrode wear rates at several different operating conditions and modes in multiple tests at JPL. The single emitter electro spray assembly is in Fig. 9. It will be installed in a temperature controlled can and maintained at 25 +/-2 °C. EMI-Im propellant will be dried to <150 ppm of water and then pressure fed from a reservoir through fused silica capillary tubing to the emitter as shown in Fig. 9. The tests will be conducted in a 2 m diameter and length high vacuum chamber at < 5x10⁻⁶ Torr in a class 100 cleanroom. The beam target includes a 3-D printed porous aluminum geometric black body (GBB) beam collector biased to -100 V and a tungsten screen biased to -200 V. This beam target has been demonstrated to absorb the EMI-Im propellant electro sprayed at it well and mitigate the backflux of propellant and electrons to the thruster when properly biased to negligible levels. The tests are automated under computer control using a data acquisition system with safe automated shutdown in case of test apparatus or facility anomalies. Ultraviolet power supplies provide high voltage for electro spray control. Currents are measured at the high-voltage electrodes, using a shunt resistor and an isolation amplifier for transferring this small voltage signal to laboratory ground.

In these experiments the mass change of the extractor and accelerator will be measured after hundreds of hours of operation in steady and unsteady transient modes expected in flight. Preliminary test conditions are in Table 1. A single emitter extractor electrode is in Fig. 10 and the accelerator is in Fig. 11. The measurement resolution of the analytical balance is 10 micrograms. These tests must be conducted long enough for the propellant mass deposition in the electrodes to significantly exceed the measurement resolution. At least 2 steady mode tests will be conducted at 250, 350 or 550 nA with clean electrodes to represent Beginning of Life conditions (BOL) and with the electrodes >90% full of propellant to represent End Of Life conditions (EOL). 2-3 transient mode tests will be conducted with 1) continuous on/off cycling, with 2) continuous cycling through the nominal operating range and/or with 3) limited operation with bubbles expected with first start during commissioning in flight as the propellant absorbs any water from the walls of the feed system flow channels to the emitter tips. The currents to all of the electrodes will be measured throughout the test. A Temperature Controlled Quartz Crystal Microbalance (TQCM) will be mounted at the electro spray source facing the beam target to measure the mass flux of propellant from the beam target towards the thruster to differentiate the mass in the extractor and accelerator from the beam and from the beam target during the tests.



Figure 9. Single electro spray emitter assembly.

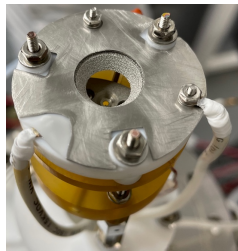


Figure 10. Single emitter assembly porous extractor.

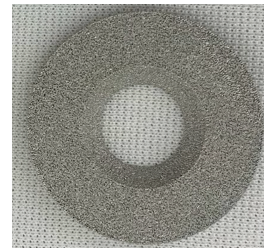


Figure 11. Single emitter assembly porous accelerator

Table 1. Table of preliminary single emitter test operating point goals and rationale for duration and cycles. The test conditions are not yet prioritized. Test conditions are under development, and each test will inform the next test condition and priority.

Test	Current or Operating Mode	Duration (hours)	Cycles	Rationale and expected mass deposition
1	250 nA, 2kV at BOL	200*		>30 μg propellant deposition (extractor) >30 μg propellant deposition (accelerator)
2	350 nA, 6 kV at BOL	300*		>30 μg propellant deposition (extractor) >30 μg propellant deposition (accelerator)
3	550 nA, 6 kV at BOL	500*		>30 μg propellant deposition (extractor) >30 μg propellant deposition (accelerator)
4	Wet propellant bubble mode	72+*		>3 days of operation with bubble shedding on start up is possible
5	Starts and stops		1000	Exoplanet observatories expect >1000 observations over 5 years [6]
6	Continuously changing (10 Hz) thrust level at 1.7 μN +/- 0.3	300+*		Typical operation expected in science mode for precision pointing an observatory
7	350 or 250 nA at EOL	300*		Characterize EOL performance and mass change at 93% full, >30 μg propellant deposition (extractor) >30 μg propellant deposition (accelerator)

* lower duration tests may result in successful mass change measurements with acceptable error.

4.2 Beam Measurements

Experiments with a single emitter electrospray assembly with the CMT electrode geometry will be conducted at UCI to measure jet velocity and potential for the beam model in the life model. The electrospray source is operated inside a vacuum chamber, needed to characterize its beams with time-of-flight and retarding potential analyzers. Fig. 12 is a sketch of the experimental setup. The emitter is the chamfered and metallized end of a fused silica tube with an outer diameter of 360 μm , an inner diameter of 40 μm , and a length of 0.688 m. The opposite end exits the chamber through a vacuum fitting, and is submerged in a vial with EMI-Im placed at the bottom of a hermetic glass bottle. A cylinder with pressurized argon, a mechanical pump, a pressure gauge, and a manifold with a system of valves are used to control the pressure in the bottle and feed the desired amount of EMI-Im to the emitter. The hydraulic resistance of the fused silica line was calibrated with a bubble flow meter, which confirmed the validity of using the Poiseuille law with the nominal length and inner radius of the line to determine the liquid flow rate Q from the applied pressure. During operation, a roughing mechanical pump and a turbomolecular pump bring the pressure in the vacuum chamber down to 2×10^{-6} Torr. The current emitted by the electrospray is measured in the high-voltage line powering the emitter, using a shunt resistor and an isolation amplifier for transferring this small voltage signal to laboratory ground.

The average velocity of the droplets at the jet breakup point, v_j , and the electric potential at this point with respect to ground, ϕ_j , are measured with a differential retarding potential analyzer (an electrostatic mirror) and a time-of-flight (TOF) analyzer operated in tandem [21], as shown in Figs. 12 and 13. The mirror, with a voltage difference VRP between plates, filters the incoming particles by retarding potential and only those with $\phi_{RP} = \text{VRP}$ are transferred through. The distance between the entry and exit orifices, the gap between the plates, the plate thickness, and the diameter of the orifices are 5.08 cm, 2.54 cm, 0.95 cm, and 1.58 mm, respectively. The current of the particles exiting the mirror and striking a small collector is measured with a fast electrometer. The collector is 15.6 cm downstream from an electrostatic gate placed at the exit of the mirror, which is L_{TOF} . When the electrostatic gate is off and VRP is swept the electrometer yields the retarding potential density distribution $dI/d(\phi_{RP})$. When the gate is rapidly turned on at fixed VRP to deflect the beamlet, the electrometer yields the time-of-flight distribution across the

drift tube. With both ϕ_{RP} and L_{TOF} precisely known, this instrument provides an accurate mass-to-charge distribution.

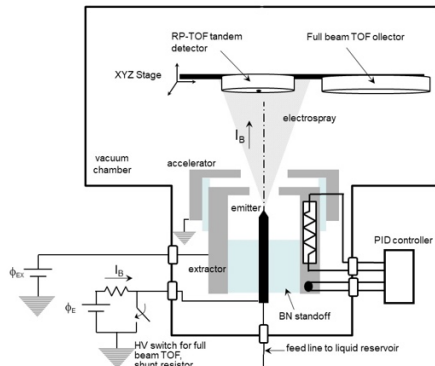


Figure 12. Experimental setup: electro spray source, vacuum chamber, and detectors.

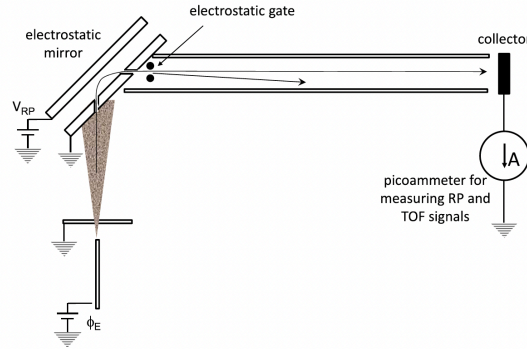


Figure 13. Retarding potential (electrostatic mirror) and time-of-flight analyzers operated in tandem.

4.3 Thruster Electrode Wear Rate Measurement and Lifetime Estimate

The thruster life test will be conducted to validate the thruster design at Busek. The test includes the 9 emitter thruster in Fig. 3, the propellant flow control assembly and the propellant tank. The thruster and flow control assembly will be integrated in a housing box with temperature control. The power electronics including high voltage power supplies and electrode current measurement electrometers will be integrated with a data acquisition and control system for unattended operation and safe test shutdown in case of any test apparatus or power anomalies. The test facility includes a 1.5 m vacuum chamber with cryopumps to maintain high vacuum at $<5e-6$ Torr. A JPL-designed, porous aluminum GBB beam target will be built and installed above the vertically oriented thruster to capture the propellant to mitigate backspray and splashing from the facility to the thruster.

The life test will be conducted at multiple operating points through the performance range to characterize performance stability and electrode wear rates. The mass of the extractor and accelerator electrodes will be measured before and after the test to verify acceptable wear rates and valid thruster design. The CMT extractor is shown in Fig. 14, and the accelerator is shown in Fig. 15. The test operating conditions for the 4000-8000 hour life test are under development. The test data will be reviewed periodically to determine if the test and thruster are operating as necessary to continue. Throughout the test, current to each electrode will be measured to monitor stability and estimate mass deposition rates and total mass accumulation. Mass flux from the beam target towards the thruster will be measured with a Temperature-controlled Quartz Crystal Microbalance (TQCM) to estimate the mass deposited in the electrodes from the beam target during the test.



Figure 14. CMT extractor electrode.

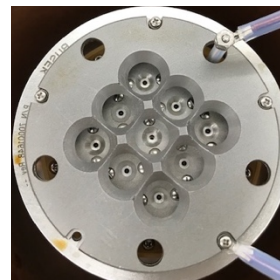


Figure 15. CMT accelerator electrode.

5 Data Measurement & Analysis

5.1 Single Emitter Assembly Electrode Wear Rates

Single emitter tests will be conducted to measure extractor and accelerator electrode mass loading rates at multiple conditions (Eqn.11) including steady current levels and unsteady transient conditions. Preliminary test condition goals are in Table 1. The electrode mass change measurements will be compared to the thruster life model predictions for model validation.

$$\dot{m}_{ex,ac} = \frac{\Delta m_{ex,ac}}{\Delta t} \quad (11)$$

Average specific charge, $\langle q/m \rangle_{ex}$ and $\langle q/m \rangle_{ac}$, for the current of charged particles to the electrodes (Eqn. 12) can be estimated from the electrode current measurements, I_{ac} and I_{ex} , throughout the test and the mass change measurements after the test.

$$\langle \frac{q}{m} \rangle_{ex,ac} = \frac{\int_0^{t_{test}} I_{ex,ac} dt}{\Delta m_{ex,ac}} \quad (12)$$

Estimating the beam current oversprayed to each of the electrodes and the mass deposited into them requires correcting for other contributions to the currents measured that include secondary charged particles from the high energy charged droplet and molecular ion impacts with electrodes. They can splash, spray and evaporate propellant species that are neutral and positively and negatively charged. The currents can be estimated by solving equations of charge conservation at each of the electrodes with measurements and estimates for secondary species yields. [9] Estimated currents from the beam to the extractor and accelerator for a beam voltage of 6 kV are in Fig. 16. The extractor and accelerator currents can be used with the average specific charge of the charged particles in those currents to estimate the mass transport to the electrodes and to estimate the impact of operating at that current level on lifetime. Beam modeling results suggest that the beam charged particle specific charge is 9048 C/kg at high angles where the beam is intercepted by the extractor and accelerator electrodes [9]. The results of a long duration test of a single emitter at 350 nA and 6 kV with electrode mass change and current measurements suggest that the average specific charge of charged particles in the beam current to the extractor is 641 C/kg and it is 1241 C/kg in the beam current to the accelerator. It was higher than the average specific charge in the primary beam, which is 530 C/kg at 350 nA. These preliminary specific charge values can be used to estimate the electrode loading rates from the current measurements, as shown in Fig. 16, and the duration of a test required to accumulate enough propellant to significantly exceed the measurement resolution, as done for the test duration and mass change estimates provided in Table 1. Fig. 16 shows measured single emitter assembly electrode currents with emitter current and the corresponding propellant mass flow rates for the range of expected charged particle specific charge. The goals for more than 7.5 years of operation is represented by the green curve for a single emitter contribution in a 9 emitter thruster considering the electrode capacity. The two vertical black lines on each of the graphs in Fig. 16 bound the single emitter nominal current range, where the thruster could operate for more than 7.5 years.

Once the specific charge is determined at specific current levels in the single emitter tests, they can be used with corrected electrode current measurements in the thruster test to estimate the mass deposition rates, \dot{m}_{ex} and \dot{m}_{ac} , at those current levels (Eqn. 13), and total deposited mass, improving on the range estimates in Fig. 16. They will enable estimates of the mass accumulation during the long duration test to compare to both the final mass change measurements and the modeling results.

$$\dot{m}_{ex,ac} = \frac{I_{ex,ac}}{\langle \frac{q}{m} \rangle_{ex,ac}} \quad (13)$$

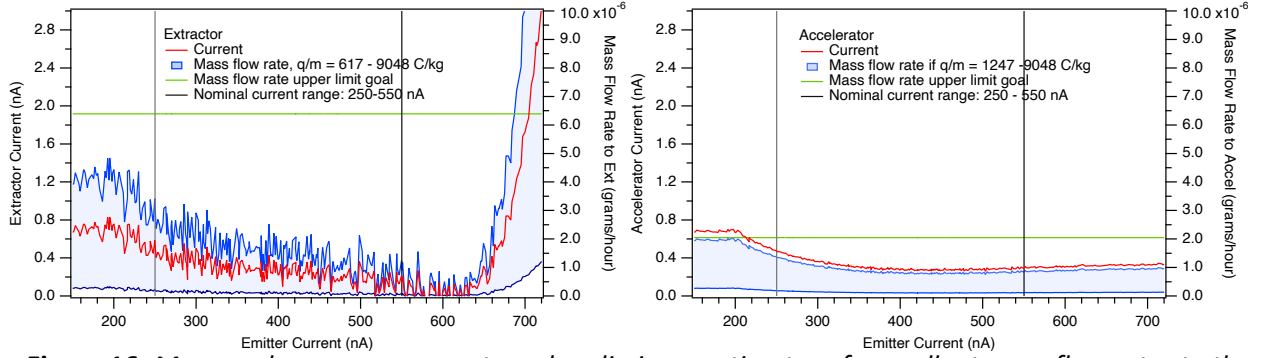


Figure 16. Measured overspray currents and preliminary estimates of propellant mass flow rates to the extractor and accelerator electrodes with emitter current for an emitter voltage of 6 kV for the range of specific charge expected based on modeling and experimental results.

5.2 Beam Measurements

The velocity of the charged droplets and the electric potential at the jet breakup are initial and boundary conditions for the electro spray beam model. These measurements are required throughout the CMT single emitter current range and operating temperatures with EMI-1m propellant. The distribution of charge-to-mass ratio and retarding potentials typical of electro spray droplets enable estimating the jet potential and velocity at its breakup from these two measurements [19,27]. The charged particle mass-to-charge ratio distribution can be measured accurately with the tandem retarding potential and time-of-flight analyzers illustrated in Fig. 14 and 15. The mirror, with a voltage difference VRP between plates, filters the incoming particles by retarding potential and only those with $\phi_{RP} = VRP$ are transferred through [Error! Bookmark not defined.]. The current of the particles exiting the mirror and striking a small collector is measured with a fast electrometer. When the electrostatic gate is off and VRP is swept the electrometer yields the retarding potential density distribution $dI/d(\phi_{RP})$. When the gate is rapidly turned on at fixed VRP to deflect the beamlet, the electrometer yields the time-of-flight distribution across the drift tube. With both ϕ_{RP} and L_{TOF} precisely known, this instrument provides an accurate mass-to-charge distribution measurement. The mapping between mass-to-charge ratio ζ , retarding potential ϕ_{RP} , particle travel length L_{TOF} , and time of flight τ_{TOF} is

$$\zeta = 2\phi_{RP} \left(\frac{\tau_{TOF}}{L_{TOF}} \right). \quad (14)$$

The nominal velocity v_j and potential ϕ_j of the jet in the breakup region can be determined from measurements of ζ and ϕ_{RP} . The technique is based on the natural dispersion of the droplets' mass-to-charge ratio induced by the breakup, and assumes that the variations of potential and droplets' velocities in the unsteady breakup region are much smaller than the voltage drop along the cone jet and the velocity gained by the liquid along the jet. Under these conditions all droplets produced by the breakup are emitted at approximately the same nominal potential ϕ_j and velocity v_j . Thus, if the retarding potentials and mass-to-charge ratios of many "i" droplets emitted from the breakup region are available, ϕ_j and v_j can be obtained from the linear regression [27]

$$\phi_{RP,i} = \frac{1}{2} v_j^2 \zeta_i + \phi_j. \quad (15)$$

5.3 Thruster Electrode Wear Rate Measurement and Lifetime Estimate

The extractor and accelerator mass will be measured before and after the long duration test to determine the mass change. The expected mass change of the extractor and accelerator electrodes during an 8000 hour test is expected to be >10 mg from operation in the nominal thrust range during the test. The propellant contribution from the unsteady modes is not yet predictable. It should be predictable after the single emitter tests in unsteady modes. With an analytical balance mass measurement resolution

of 0.1 mg, the measurement error will be < 1% of the measurement after 8000 hours and < 2% after 4000 hours.

The mass flux at the thruster from the beam target will be measured throughout the test to estimate the mass deposited on the extractor and the mass deposited on the accelerator electrodes from the beam target. The mass flux back from the beam target depends on the beam target configuration, collector and screen biasing, beam current, beam voltage and surface coverage with propellant; therefore, it must be measured throughout the entire test. Propellant backflux measurements with a similar beam target in single emitter tests at JPL suggest that < 4 mg will be deposited to the extractor and <16 mg will be deposited to the accelerator during 8000 hours of thruster operation. The mass deposited from the beam target will be subtracted from the electrode mass change measurements to determine the electrode propellant mass change that would be expected from the beam in flight. The mass changes from the beam must be commensurate with a 7.5+ year thruster lifetime to validate the thruster technology.

Determining the remaining thruster lifetime will require an understanding of the electrode wear rates in each operating mode from the single emitter tests that have been applied to estimate the mass change in the long duration test with reasonable agreement. The currents to the extractor and accelerator electrodes will be measured throughout the test to monitor stability and to estimate the mass loading rates, as estimated for the data in Fig. 15, with improved average specific charge estimates for lower rate uncertainties. The first start up with bubble shedding is expected to result in the highest propellant flow rates to the electrodes. That operating mode will only be at the first start-up during commissioning. The remaining thruster lifetime will be estimated for 1000 additional stops and restarts and then operation in the nominal thrust range in science mode, based on the single emitter test results and the validated life model results.

5.4 Lifetime Model Validation

The lifetime model mass change prediction must agree with the experimental results from the single emitter and thruster test within the quantified uncertainty of the model to 1- σ for validation. The lifetime model will be applied to predict the mass changes for each of the steady current single emitter tests for validation with agreement within 1- σ before it is applied to predict the electrode mass changes during the long duration thruster test. The lifetime model will be run for the exact test conditions to predict the change in mass of the electrodes for comparison against the experimental results.

5.5 CMT Design Validation

A life model simulation will be conducted with the validated model for an observatory mission thruster thrust profile to demonstrate a 7.5 year lifetime with 95% confidence interval considering the expected time in transient modes and science mode at 5-30 μ N to validate the thruster technology for it. Since the thruster technology scalability will also be demonstrated, the simulation could be conducted for any required thrust level to determine the number of emitters and extractor and accelerator mass capacity for the required thrust level and lifetime.

6 Success Criteria

- 6.1 Single electrospray emitter tests in multiple steady and transient operating modes at BOL and at EOL conditions with measured mass changes of the extractor and accelerator electrodes from propellant deposition with results that are commensurate with a 7.5 year lifetime by demonstrating that the combined mass from the measured propellant mass deposition rate and expected time in each mode for a relevant mission and thrust profile for a single emitter projected to a 9-emitter thruster can be accommodated by the mass capacity of the thruster electrodes.**

Rationale: Propellant overspray onto and filling the porous electrodes is the primary wear process. The propellant mass change in the electrodes will be measured to estimate the propellant mass flow rate to them to verify acceptable rates that are commensurate with a 7.5 year lifetime. These measurements will be compared against the life model results to validate the life model at each steady current level tested. The current measurements with the mass change measurements will enable an estimate of the average specific charge of the charged particles to the electrodes at each current level. The specific charge can be used to estimate the propellant mass flow rate to the electrodes from the current measurements during the long duration thruster test and predict mass changes independent of the life model to assess the scalability of the single emitter wear rate measurements to the thruster wear rate measurements. The propellant mass flow rates to the electrodes during unsteady transient modes have never been measured. It is critical to have these data to verify acceptable wear rates and to estimate the thruster lifetime. They will be applied to the life test analysis to estimate mass deposition during transient modes and remaining lifetime. These data are necessary to estimate thruster lifetime for any mission thrust profile. These measurements will verify acceptable electrode wear rates at expected unsteady/transient modes of operation.

- 6.2 An independent review board certifies the long duration thruster test plan, operational approach, and facility as ready to begin the test, prior to start of testing.**

Rationale: This review will improve the probability of success of the long duration test.

- 6.3 Long duration multi-emitter thruster wear test for 4000-8000 hours to demonstrate confidence in the thruster design and lifetime model prediction by 1) demonstrating controllable and predictable performance, 2) revealing a deposited mass of propellant in the extractor and accelerator electrodes during the test with multiple mission-relevant transient and steady operating modes that is in agreement with model predictions within a 1- σ confidence interval and 3) with a remaining mass capacity in the electrodes to accommodate the expected propellant loading that the lifetime model predicts for a relevant mission thrust profile and number of on-off cycles during more than 61,700-57,700 hours of additional science mode operations to 7.5 years. The required remaining capacity of the extractor after the long duration test is currently estimated to be 55% (after 4000 hours) or 52% (after 8000 hours) and the accelerator should exceed an estimated 49% (after 4000 hours) or 46% (after 8000 hours) at the end of the test.**

Rationale: Stable and predictable performance is required in a long duration thruster test with multiple emitters if it is going to be necessary for 65,700 hours (7.5 years) and to demonstrate scalability of the technology. 8000 hours will result in electrode mass changes that can be measured with a <1% error. 4000 hours may also result in electrode mass changes that can be measured with a <1% error. 4000 hours is longer than the longest previous CMT life test and 8000 hours is more than 2X the longest previous CMT test. An 8000 hour test is the longest test expected to be achievable within the task resources.

6.4 Life model validation with test results with agreement within 1-σ confidence interval.

Rationale: *This result is required for successful model validation.*

7 Certification

The PI will prepare a milestone certification package for review by the ExEPTAC and the ExEP program. In the event of a consensus determination that the success criteria have been met, the project will submit the findings of the review board, together with the certification package, to NASA HQ for official certification of milestone compliance. In the event of a disagreement between the ExEP project and the ExEPTAC, NASA HQ will determine whether to accept the data package and certify compliance or request additional work.

7.1 Milestone Certification Data Package

The milestone certification data package will contain the following explanations, charts and data products.

- 7.1.1 A narrative report, including a discussion of how each element of the milestone was met, and a narrative summary of the overall milestone achievement.
- 7.1.2 A description of each of the single emitter test measurement results.
- 7.1.3 A description of the beam model and the validation results.
- 7.1.4 A description of the lifetime model and the validation results.
- 7.1.5 A description of the thruster long duration test and the test results.
- 7.1.6 A discussion on the thruster lifetime assessment results.
- 7.1.7 Thruster lifetime modeling results for a mission application.

8 Schedule

A schedule is provided in Fig. 17 for the high level tasks and progress reviews.

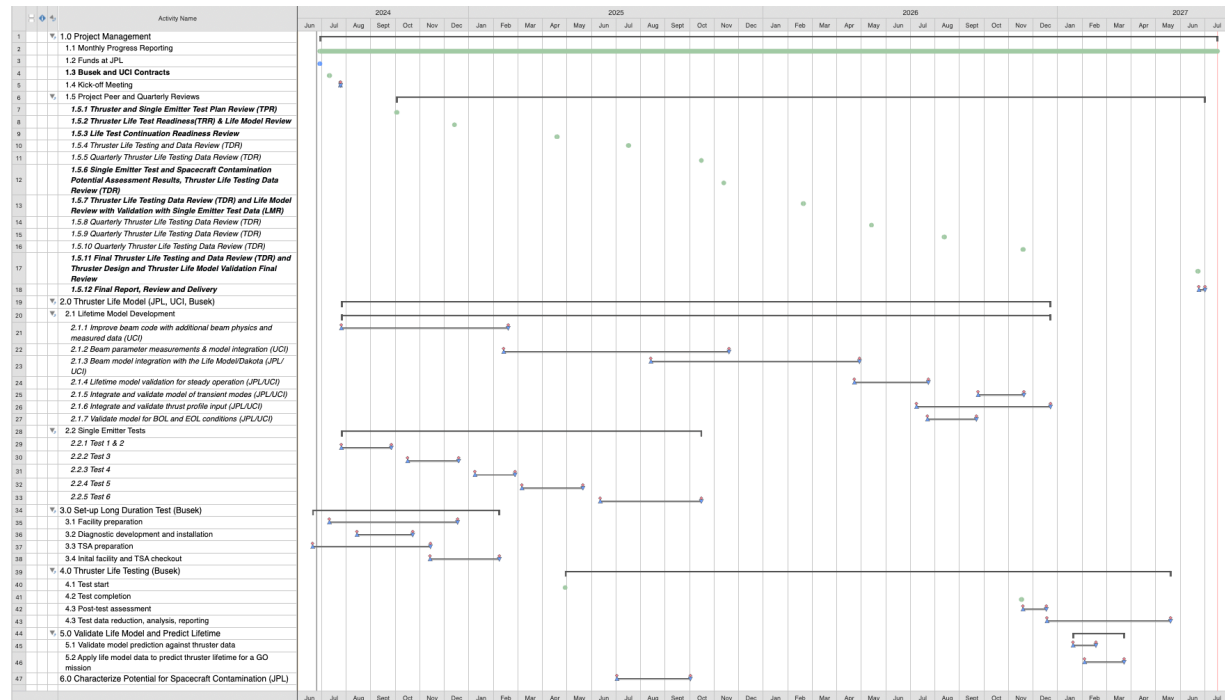


Figure 17. Schedule of tasks and reviews. The reviews in bold font represent important milestones.

9 Acknowledgements

This work was carried out at the Jet Propulsion Laboratory, California Institute of Technology, under a contract with the National Aeronautics and Space Administration (80NM0018D0004).

10 References

1. Decadal Survey: Pathways to Discovery in Astronomy and Astrophysics for the 2020s (2021), Astro2020.
2. Ziemer, J. K., et al., "In-Flight Verification and Validation of Colloid Microthruster Performance," AIAA 2018-4643.
3. Anderson, G., et. al., "Experimental results from the ST7 mission on LISA Pathfinder," Phys. Rev. D 98, 102005 (2018).
4. B. Scott Gaudi et al., "HabEx: Habitable Exoplanet Observatory Final Report (2019)".
5. Dennehy, C. J., et al. "Application of Micro-Thruster Technology for Space Observatory Pointing Stability," NASA/TM-20205011556, NESC-RP-18-01375.
6. Haag, C., Balachandran, K., Alvarez-Salazar, O., Marrese-Reading, C., Arestie, S., Warfield, K., "Microthruster ACS Architecture for Precision Pointing of 6 Meter Exo-Earth Imaging Space Telescope," AAS 24-073.
7. Hruby, V., et al. "ST7-DRS Colloid Thruster System Development and Performance Summary," AIAA 2008-4824.
8. Ziemer, J. K., et al., "Colloid Microthruster Flight Performance Results from Space Technology 7 Disturbance Reduction System," IEPC 2017-578.
9. Marrese-Reading, C., et al., "Electrospray Thruster Lifetime Modeling with Uncertainty Quantification and Experimental Validation", IEPC Paper No. 2022-234, 37th International Electric Propulsion Conference, 2022.
10. Gamero-Castano, M., Hruby, V., "Electrospray as a source of nanoparticles for efficient colloid thrusters," J. Propul. Power 17, 977 (2001).
11. Gamero-Castano, M., "Characterization of the electrosprays of 1-ethyl-3methylimidazolium bis(trifluoromethylsulfonyl)imide in vacuum," Phys. Fluids 20, 032103.
12. Magnani, M. & Gamero-Castaño, M., "Numerical Simulation of Electrospraying in the Cone-Jet Mode", Journal of Fluid Mechanics, 859 (2019)
13. Ziemer, J., "Performance of Electrospray Thrusters," IEPC-2009-242, 31st International Electric Propulsion Conference, Ann Arbor, MI, September 20-24, 2009.
14. Ziemer, J., et al., "Flight Hardware Development of Colloid Microthruster Technology for the Space Technology 7 and LISA Missions," 30th International Electric Propulsion Conference, IEPC-2007-288, Florence, Italy, September 2007.
15. Demmons, N., et. al., "ST7-DRS Mission Colloid Thruster Development," 2008-4823, 44th AIAA Joint Propulsion Conference, Hartford, CT, July 2008.
16. Marrese-Reading, et al, "ST7 Disturbance Reduction System (DRS) Colloid Micronewton Thruster Performance and Control Algorithm Model Simulation Validation In Flight," JANNAF 2018 – 5743.
17. Galobardes-Esteban, M., Cisquella Serra, A., Gamero-Castano, M., "A Hybrid Model for Beams of Droplets and Ions of Electrospray Thrusters," IEPC-2022-236.
18. Gamero-Castaño, M., "The structure of electrospray beams in vacuum." Journal of Fluid Mechanics 604 (2008): 339-368. doi: 10.1017/S0022112008001316
19. Gamero-Castaño, M., Hruby, V., "Electric measurements of charged sprays emitted by cone-jets." Journal of Fluid Mechanics, 459 (2002), 245-276
20. Gamero-Castaño, M., "Retarding potential and induction charge detectors in tandem for measuring the charge and mass of nanodroplets." Review of Scientific Instruments, 80, 053301/1-4, 2009

-
21. Gamero-Castano, M., and Cisuella-Serra, A., "Electrosprays of highly conducting liquids: A study of droplet and ion emission based on retarding potential and time-of-flight spectroscopy," *Phys. Rev. Fluids* 6, 013701 (2021).
 22. Ziemer, J. K., et al, "Progress on LISA Colloid Microthruster Technology Development," AIAA 2020-3609.
 23. Wirz, R. E., et al., "Electrospray Thruster Performance and Lifetime Investigation for the LISA Mission," AIAA 2019-3816.
 24. Eldred, M. S. et al., "DAKOTA, A Multilevel Parallel Object-Oriented Framework for Design Optimization, Parameter Estimation, Uncertainty Quantification, and Sensitivity Analysis," Version 3.1 User's Manual, Sandia Technical Report SAND2001-3796, Revised April 2003, Sandia National Laboratories, Albuquerque, NM.
 25. Demmons, N. et al., "Life-Limiting Factors of the CMTS for Precision Pointing Observatory Missions," AIAA 2021-3403.
 26. Collins, A. L., Uchizono, N.M., Huh, H., Wirz, R. "Three-Dimensional Microscopy and Analysis of the Emission Cone Meniscus for Electrospray Thrusters", IEPC 2022-228.
 27. Gamero-Castaño, M., "The structure of electrospray beams in vacuum," *J. Fluid Mech.* 604, 339 (2008).